ARTÍCULO ORIGINAL

TIP Revista Especializada en Ciencias Químico-Biológicas, 22: 1-18, 2019.
DOI: 10.22201/fesz.23958723e.2019.0.171

Microbialite-dominated fossil associations in Cipit Boulders from Alpe di Specie and Misurina (St. Cassian Formation, Middle to Upper Triassic, Dolomites, NE Italy)

Francisco Sánchez-Beristain[1]* and Joachim Reitner[2]
[1]Museo de Paleontología, Facultad de Ciencias, Universidad Nacional Autónoma de México. Circuito Exterior S/N. Ciudad Universitaria. Coyoacán 04510. Ciudad de México, México. [2]Geowissenschaftliches Zentrum der Universität Göttingen, Abt. Geobiologie, Goldschmidtstraße 3. 37077 Göttingen, Germany.
E-mail: *sanchez@ciencias.unam.mx

Abstract
In this paper we describe four new fossil associations of "reef" and "reef"-like environments of the St. Cassian Formation (Ladinian-Carnian, Dolomites, NE Italy), based on thirty thin sections from 10 "Cipit boulders" olistoliths, which slided from the Cassian platform into coeval basin sediments. The fossil associations were determined by means of microfacies analysis using point-counting and visual estimation, as well as with aid of statistical methods, based on all fractions with a biotic significance (biomorpha and microbialites). Cluster Analyses in Q-Mode were performed, coupling three algorithms and two indices. In all samples, the main components of the framework are microbialite (average of 75%), and macrofossils (average of 20%), whereas cements and allochtonous components, such as allomicrite, do not represent a significant fraction.
Based on both microbialite and fossil content, Chaetetid–microencruster Association, Microbialite–microencruster Association, Dual-type Microbialite Association and Microbialite–*Terebella* Association, were differentiated. The palaeoenvironmental settings where the associations come from are separately discussed. Microencrusters helped determine energy and luminosity settings. Microencruster abundance and diversity, in addition to the conspicuousness of microbialite, indicate that all associations come either from a deep, or from a cryptic setting.
Key words: Microbialite associations, Microencrusters, Cluster analysis, olistoliths, St. Cassian-Formation – Triassic, Dolomites.

Asociaciones fósiles dominadas por microbialita provenientes de los olistolitos Cipit de Alpe di Specie y Misurina en la Formación San Cassiano (Triásico Medio - Superior, Dolomitas, NE de Italia)

Resumen
En este trabajo se describen cuatro nuevas asociaciones fósiles provenientes de la Formación San Cassiano (Ladiniense–Carniense, Dolomitas, NE de Italia), basándonos en treinta láminas delgadas elaboradas a partir de 10 calizas Cipit. Éstas son olistolitos que se desprendieron de las plataformas Cassianas hacia sedimentos contemporáneos de cuenca, siendo así relictos de ambientes "arrecifales", o similares a arrecifes. Todas las muestras provienen de la *Fossillagerstätte* de San Cassiano. Las asociaciones fósiles fueron determinadas por medio de análisis de microfacies utilizando conteo de puntos y estimación visual y con ayuda de métodos estadísticos, tomando como base todas las fracciones con una importancia biológica (biomorfos y microbialitas). Se efectuaron análisis de clústeres en modo Q, acoplando tres algoritmos y dos índices. En todos los análisis, las principales fracciones son microbialitas (en promedio 75%) y macrofósiles (un promedio del 20%), en tanto que los cementos y aloquímicos, como alomicrita no representan una fracción importante en los análisis estadísticos.
Las asociaciones obtenidas fueron nombradas como se enuncia a continuación: Asociación quetétido–microencostrante, Asociación microbialita–microencostrante, Asociación microbialítica dual y Asociación Microbialita–*Terebella*, respectivamente. Las características del paleoambiente del que provienen las asociaciones son discutidas por separado, tomando como base el contenido fósil y de microbialita. Los microencostrantes fueron de gran utilidad para la determinación de las condiciones de energía y luminosidad. Los resultados, considerando tanto la abundancia y diversidad de microencostrantes, en conjunto con la conspicuidad de microbialitas, indican que todas las asociaciones provienen de un ambiente profundo o de uno críptico.
Palabras clave: Asociaciones microbialíticas, Microencostrantes, Análisis de clústers – Olistolitos, Formación San Cassiano, Triásico , Dolomitas

Nota: Artículo recibido el 05 de noviembre del 2018 y aceptado el 25 de febrero del 2019.

DOI: 10.22201/fesz.23958723e.2019.0.171

Introduction

Microbialites are known to have contributed significantly to "reef" and "reef"-like structures in the past as well as in the present (e.g. Wood, 1999, 2001; Saint-Martin, Müller, Moissette & Dulai, 2000; Olivier *et al.*, 2004; Nose, Schmid & Leinfelder, 2006; Westphal, Heindel, Brandano & Peckmann, 2010). Disregarding the fact whether they are able or not to form ecological reefs *sensu stricto* (Fagerstrom, 1987) by themselves, (e.g. Neuweiler, 1993; Webb & Kamber, 2000; Neuweiler & Bernoulli, 2005; Floquet, Neuweiler & Léonide, 2012; Heindel *et al.*, 2012; Duda *et al.*, 2016), their role in bulding "mud mound"-like structures has been recognised since the nineties of the last century and up to date (Reitner & Neuweiler, 1995; Dupraz & Strasser, 2002; Chan *et al.*, 2014). They may reach important percentages (more than 50%) in ancient frameworks, particularly after extinction events; most notably in the Precambrian–Cambrian transition (Zhuravlev, 1996; Turner, Narbonne & James, 2000; Shapiro, 2004; Wahlman, Orchard & Buijs, 2013), the Permian–Triassic boundary (Delecat & Reitner, 2005; Ezaki, Liu, Nagano & Adachi, 2008; Kershaw, 2017); and the Cretaceous–Paleogene boundary (Zamagni, Kosir & Mutti, 2009; Tunis *et al.*, 2011; Astibia, López-Martínez, Elorza & Vicens., 2012). They can also dwell successfully in deep and in cryptic environments, where the influence of light is minimum, or none at all (Keupp & Arp, 1990; Reitner, 1993; Reitner, Wilmsen & Neuweiler, 1995; Webb & Jell, 1997; Guido *et al.*, 2017).

Microbialites have often been identified in the deposits of the famous *Fossillagerstätte* St. Cassian Formation. They are particularly abundant in the Cipit boulders in Seelandalpe (Alpe di Specie) and Misurina (Trentino-Alto Adigio, South Tyrol, NE Italy). These olistoliths come from the Cassian platforms, and have escaped late diagenetic processes due to their swift deposition in basin areas (Fürsich & Wendt, 1977; Wendt & Fürsich, 1980; Bosellini, 1991; Russo, Neri, Mastandrea & Laghi, 1991). Microbialites may account for more than 50% of any single olistolith (Russo, Neri, Mastandrea & Baracca, 1997).

Recently, Sánchez-Beristain & Reitner (2016, 2018) have described new fossil associations either dominated by metazoans or by microbialites (up to 60% of the framework), using statistical methods. However, they did not describe any association significantly dominated by traditional metazoan "reef" builders in these works. Their first work in this regard (Sánchez-Beristain & Reitner, 2016) includes five "coralline" sponge-based associations, plus one dominated by calcareous algae and hexactinellid sponges. Their second work dealing with this topic (Sánchez-Beristain & Reitner, 2018) includes four further sponge associations with a vast diversity of microencrusters. The aim of the present work is thus to determine the palaeonvironmental-palaeocological setting of the "reef" sediments forming the olistoliths, in particular those that are mainly composed by, or have an important percentage of microbialite. The detailed microfacies analysis of thin sections has allowed us to recognize three new fossil associations in the St. Cassian Formation, where microbialite accounts ca. 75%, and up to 90% of total framework, as well as a new association based on a chaetetid sponges/microencrusters and microbialites. Statistical methods proved effective in differencing similar microbialite-based associations, mainly by considering the diversity of microencrusters, which help infer palaeoenvironmental constraints. These results may be of special interest, since most Cipit boulders from the main localities where the St. Cassian Formation outcrops -namely Alpe di Specie and Misurina- are mainly dominated by a vast array of metazoans (Wendt, 1982; Sánchez-Beristain & Reitner, 2012, 2016).

Geological setting

The St. Cassian Formation (upper Ladinian–lower Carnian) crops out in the Dolomites (Figure 1). First designated by Münster (1841) and cartographically characterised by von Hauer (1858), it is constituted by an alternation of shales, marls and calciturbidites (Wendt & Fürsich, 1980), with maximum thickness between 400 and 500 m (Bizzarini & Braga, 1978). This formation consists of two members (Upper Member and Lower Member; Figure 2). Division is performed based on ammonite biozones. The *Frankites regoledanus* Zone corresponds to the Ladinian Lower Member deposits, whereas the *Daxatina*

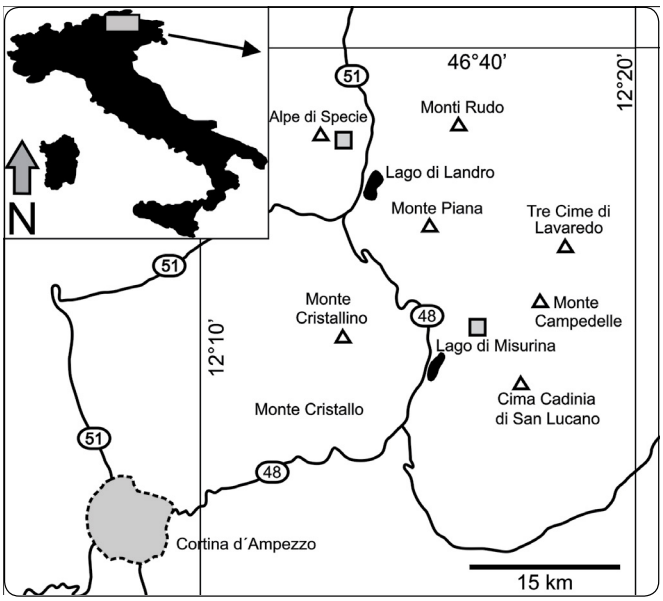

Figure 1. Geographic position in northeastern Italy of the two localities (grey squares) where olistolith samples have been collected: the Alpe di Specie (Seelandalpe) and Misurina. Modified from Nützel, Joachimski & López-Correa (2010) and Sánchez-Beristain & Reitner (2016).

DOI: 10.22201/fesz.23958723e.2019.0.171

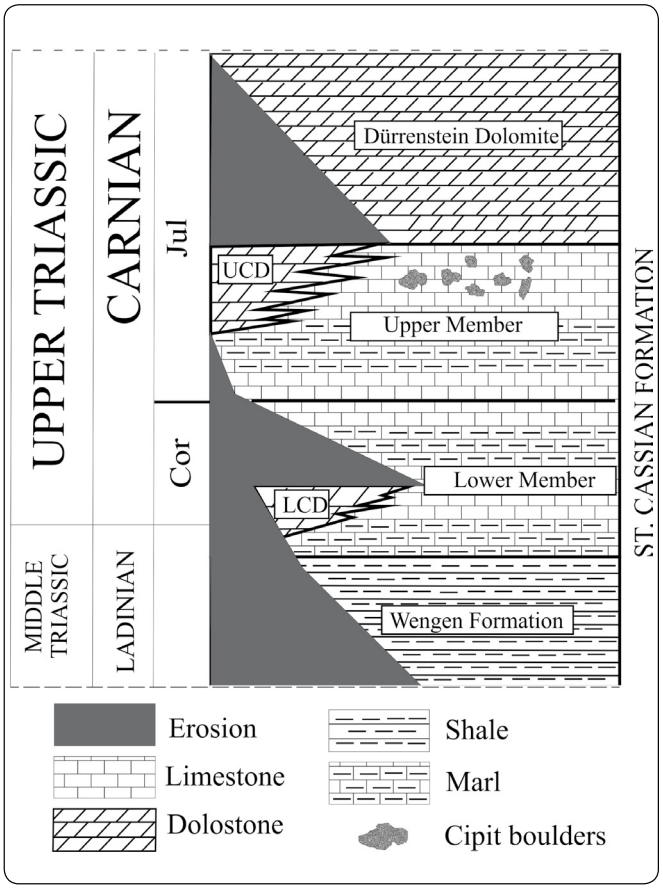

Figure 2. Chronostratigraphic distribution of the upper Ladinian to lower Carnian lithostratigraphic units in the Dolomites, NE Italy, including the studied "Cipit boulders" olistoliths in the St. Cassian Formation (LCD = Lower Cassian Dolomite; UCD = Upper Cassian Dolomite; Cor = Cordevolian; Jul = Julian). Modified from Müller-Wille & Reitner (1993) and Sánchez-Beristain, López-Esquivel Kranksith, García-Barrera & Reitner (2013).

canadensis and *Trachyceras aon* Zones correspond to the Lower Member deposits of the Cordevolian. In turn, the *Trachyceras aonoides* Zone is correlated with the Upper Member, in the Julian (Mietto *et al.*, 2012).

Both members have the same lithological composition and are partly lateral equivalents of the Cordevolian-Julian deposits of the so-called Cassian carbonate platforms (Russo, 2005), informally known as "Lower Cassian Dolomite" and "Upper Cassian Dolomite" (Figure 2). According to Bosellini (1991), this phenomenon indicates sequences of regression and transgression. The St. Cassian Formation overlays concordantly the Wengen Formation (Ladinian) and underlies the Dürrenstein Dolomite (Carnian).

The Upper Member includes the so-called "Cipit boulders", olistoliths which constitute one of the most notable features of the formation. These olistoliths are relics of the "Cassian patch reefs", which could be related to both the Upper and Lower Cassian Dolomites (Wendt, 1982). Their preservation state has allowed an accurate taxonomical determination of their fossils and other analyses, such as the characterisation of diagenetic pathways (Russo, Neri, Mastandrea & Laghi, 1991), the determination of palaeotemperatures (Stanley & Swart, 1995; Nützel, Joachimski & López-Correa, 2010), the discovery of original organic matter (Neuweiler & Reitner 1995; Sánchez-Beristain, Schäfer, Simon & Reitner, 2011), and even the study of biogeochemical and further geochemical signatures (Tosti *et al.*, 2014). These olistoliths mainly crop out in the region of Trentino-Alto Adige (South Tyrol), Northeastern Italy (Figure 1), at the Seelandalpe ("Alpe di Specie"; 46°36' N, 12°12' E) near the town of Carbonin (Schluderbach) and in Misurina in the Rimbianco Valley (46°35' N, 12°15' E). The samples studied here come from these two areas and were collected by the authors of this work between the mid-eighties of the twentieth century and 2008.

The reader is referred to the works of Müller-Wille & Reitner (1993), Bosellini, Gianolla & Stefani (2003), and Sánchez-Beristain & Reitner (2012) for general and specific remarks on the stratigraphy and geology of the St. Cassian Formation.

Material and methods

Material

Thirty thin sections coming from 10 "Cipit boulders" (olistoliths) were analysed. Thin section dimensions range between 7.5 x 10 cm and 10 x 15 cm.

Microfacies and chemical analyses

We carried out microfacies analysis, which included the identification and quantification of the proportion of components in the olistoliths. Two different methods were used: visual area estimation (after Bacelle & Bosellini, 1965) and area counting (Flügel, 2010). Area counting was performed by processing each thin section with aid of an AGFA SnapScan 1236 Scanner. Thin sections were analysed microscopically, and simultaneously compared to the digitalized files on-screen. This was made in order to distinguish boundaries between different components, which allowed us to establish a graphical on-screen classification. To achieve this goal, software utilities like Metamorph (licensed to the University of Göttingen) and VistaMetrix (licensed to the first author) were used.

In order to distinguish aragonite and high-Mg calcite from ferrous calcite (frequently found in secondary cements in St. Cassian samples), all thin sections were stained with Alizarine red-S following the method by Dickson (1965), to differentiate ferrous calcite from high-Mg calcite, aragonite and dolomite (compare Sánchez-Beristain & Reitner, 2012), thus allowing us to better identify different facies types. In addition, since original organic matter can be recognised in microbialites (Neuweiler & Reitner, 1995), we performed epifluorescence microscopy

DOI: 10.22201/fesz.23958723e.2019.0.171

at some thin sections to distinguishing true organic automicrite (Reitner, 1993) from inorganic micrite.

Classification of microbialites was performed after Sánchez-Beristain & Reitner (2016), who classified microbialites into types I, II, III and IV, according to their fabric (loose peloids, densely arranged peloids, leiolite and stromatolite, respectively). The scale designed by Dupraz & Strasser (2002) was followed to quantify the abundance of all microencruster species in every thin section.

The most representative thin sections were chosen to elaborate vector graphic maps with the Corel Draw X7 software.

Microscopical observation and chemical analyses were performed at the Department of Geobiology of the GZG (Centre of Geosciences, University of Göttingen).

Statistical Analysis

The use of statistics for determining fossil associations in palaeoecology has been previously proved successful (e.g., Sepkoski, 1974; Simpson, 2007; Sánchez-Beristain & Reitner, 2016, 2018). In the present work, after quantifying all facies components in the thin sections, their corresponding values were analysed by means of statistical methods. Cluster analysis in Q-Mode was applied to all thin sections in order to group them into fossil associations. Three algorithms were used: UPGMA (Sokal & Michener, 1958), WPGMA (Sokal & Michener, 1958), and Nearest Neighbour (Legendre & Legendre, 2012). Each algorithm was coupled with the Jaccard index (Jaccard, 1912). This combination renders a presence-absence matrix of all components (organisms, microbialite, allomicrite and cements; Sánchez-Beristain & Reitner, 2016, 2018). In addition, we paired the WPGMA Algorithm with the Bray Curtis dissimilarity index. According to Bray & Curtis (1957) and Legendre & Legendre (2012), this method takes into account the individual abundance of each component in all samples.

Cluster analyses were carried out by means of the MVSP Software (1985-2009 by Kovach Computing Systems, licensed to FSB). Subsequently, the method of Sánchez-Beristain & Reitner (2016, 2018) was followed, in order to obtain the corresponding phenograms. The reason to perform a vast array of statistical algorithms was to compare their results, since both WPGMA and UPGMA emphasize in the use -or lack of use- of the arithmetic mean of all values (Sokal & Michener, 1958), while Nearest Neighbour bases on grouping clusters in an agglomerative fashion, at each step combining two clusters that contain the closest pair of elements not yet belonging to the same cluster as each other (Legendre & Legendre, 2012). Jaccard and Bray Curtis index were selected on the basis that the former takes into account similarity, while the latter rather considers dissimilarity.

Results

Microfacies Analysis

No significant difference existed between visual area estimation and area counting. In addition, five thin sections were analysed by point counting using a 1 mm-wide grid, in order to corroborate the exactness of area counting and visual estimation (Flügel, 2010). Since we did not find any difference between the results obtained by this method and the previous ones, we proceeded to interpret our results based on area counting, which is a method that combines both precision and swiftness (Bacelle & Bosellini, 1965).

The following components were identified in thin sections: fossils, microbialite, allochthonous components (detritus/allomicrite), microsparite, and cements (Tables I and II). These components have since long been identified for St. Cassian Formation samples from olistoliths, though in different percentages (e.g. Rech, 1998; Russo, 2005; Sánchez-Beristain & Reitner, 2016, 2018). Flügel (2010) included within the term *Biomorpha* all bioclasts with a high degree of preservation or articulation. Usually, microbialites are not included usually within biomorpha (Flügel, 2010). However, we decided to group them along with fossils into this category, with the aim of generating a robust palaeoecological scope in the determination

MIC	Microbialite
Dart	*Dendronella articulata*
Prc	*Precorynella* sp
Mes	*Mesophyllum* sp
Cass	*Cassianothalamia zardinii*
Epol	*Eudea polymorpha*
B-ch	Branched ceratoporellid chaetetid
Sph-C	Sphaerulitic chaetetid
Uv	*Uvanella*-like thalamides
Teth	*Tehtysocarnia cautica*
Plv	*Planiinvoluta sp*
Mcom	*Microtubus communis*
Apfr	*Alpinophragmium perforatum*
Ter	*Terebella* cf *T. lapilloides*
Tub	*Tubiphytes* cf. *T. obscurus*
Pseu	*Pseudorothpletzella*- like crusts
Ks	*Koskinobullina socialis*
Alloc	Allochthonous components
UDTD	Undetermined framework builders
MESP	Microsparite
CEM	Cements

Table I. Data of all samples analysed. See text for further details.

DOI: 10.22201/fesz.23958723e.2019.0.171

ASSOCIATION	Clustering Code	Dominating biofacies	Palaeoecological remarks
Microbialite – microencruster Association	M-m	Microbialite framework with diverse microencrusters. Metazoans insignificant. Algae rare.	Deep, low energy "mud mound" setting / Cryptic, shallow environment with low-energy levels / mid- to deep ramp low-energy microbialite- reef, oxygen-poor setting.
Dual-type Microbialite Association	2t-M	Microbialite with uniform peloid size. Metazoans rare ("chaetetid" sponges). Very seldom microencrusters. No algae. Stromatactis with several generations of cements.	Two scenarios: a) Cryptic-deep setting with a sponge-based framework and subsequent colonization by stromatolites; or 2) Initially cryptic-deep sponge-based framework with further basinward falling and recolonization by stromatolites
Chaetetid – microencruster Association	C-m	Metazoan framework with branched chaetetids and subrogate corals. Microencrusters abundant and diverse. Microbialite constituting also a major framework building fraction	Quiet, semi-cryptic/deep marine setting, probably below 50 m, similar to modern Caribbean cryptic enviroments.
Microbialite – *Terebella* Association	M-T	Framework rich in microbialite. No metazoans. Some algal patches. Deep-water microencrusters. Stromatactis with several generations of cements.	Deep "mud mound", oxygen-poor setting.

Table II. Key to all variables (cases) displayed in Table I columns. See text for further details.

of fossil reef associations, considering that both metazoans and microbialites contribute to the formation of "reef" and "reef"-like structures (Fagerstrom, 1987). Proportions (%) of all components at each thin section were input in a Microsoft Excel file (Table I). The content for each component from the microfacies analysis of all samples can be accessed through Table I, whereas their corresponding code can be seen in Table II. Selected Corel Draw schemes (Figures 3, 4) depict the most distinctive thin section of each association.

All associations were named after their most representative attributes and are summarized in Table III.

Statistical Analysis

By means of both UPGMA—Jaccard and WPGMA—Jaccard analyses (UPGMA—J and WPGMA—J on the following), four different associations were found using data from Table I. These associations are: "Chatetetid" sponge–microencruster Association (C-m), Microbialite–microencruster Association (T-M), Dual-type Microbialite Association (2tM), and Microbialite–*Terebella* Association (M-T). Associations referred were easily identifiable by their relatively medium to high J coefficient values. In UPGMA—J (Figure. 5), J values are 0.48 for M-m; 0.557 for 2tM; 0.577 for M-T and 0.684 for C-m. In the WPGMA—Algorithm (Figure 6), J values are 0.467 for M-m; 0.557 for M-T; 0.577 for 2tM, and 0.684 for C-m. Nearest Neighbour—J (NN—J) and WPGMA—Bray Curtis analyses rendered different results (Figures. 7, 8). In the case of the NN—J method (Figure 7), both the C-m and T-M phena remained robust (J = 0.77 and J = 0.556, respectively); however, all 2tM and T-M samples are grouped within a single phenon with a J = 0.6, which furthermore has three subordinate nodes at J= 0.717, J = 0.75 and J = 0.8 (Figure 7). In the case of the WPGMA—Bray Curtis analysis, the only phenon which remains intact, is C-m (Figure 8), with a BC value of 0.355. At BC = 0.345, a gross phenon groups the three remaining associations obtained by means of both UPGMA—J and WPGMA—J. A single branch containing sample M-m 6 emerges from here. A node can be found at BC = 0.23, which encompasses two further phena: one encompassing all samples from both 2tM and T-M, and a robust phenon, which groups the remaining samples from the M-m association (M-m 1 to M-m 5).

Considering that two of the procedures performed practically led to the same results (UPGMA—J and WPGMA—J), and that these two analyses show a classification based rather on the diversity of features (taxa) than in the amount of microbialite, we therefore decided to consider the associations obtained from them for the discussion and interpretation. These two types of phenograms have been successfully used in previous studies (Sánchez-Beristain & Reitner, 2016, 2018).

DOI: 10.22201/fesz.23958723e.2019.0.171

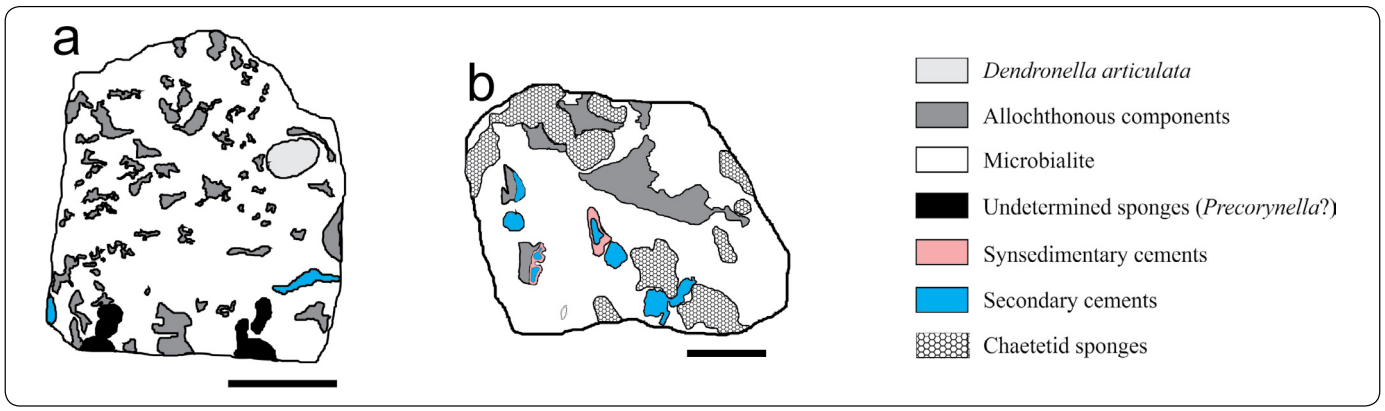

Figure 3. Microfacies maps of samples a) MI - 6 and b) MX - 5, containing the Microbialite–microencruster (M-m) association, and the Dual-type Microbialite (2tM) Association, respectively. Scale bar in a = 2.5 cm. Scale bar in b = 2 cm.

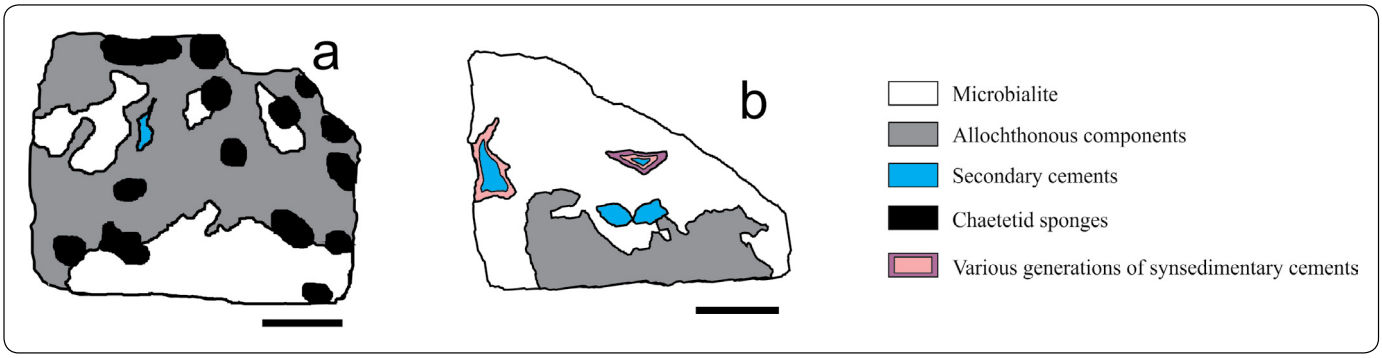

Figure 4. Microfacies maps of samples a) FSSA XXV – 3L, and b) M XL - 3, containing the Chaetetid–microencruster (C-m) Association, and the Microbialite–*Terebella* (M-T) Association, respectively. Scale bar in a = 2.5 cm. Scale bar in b = 2 cm.

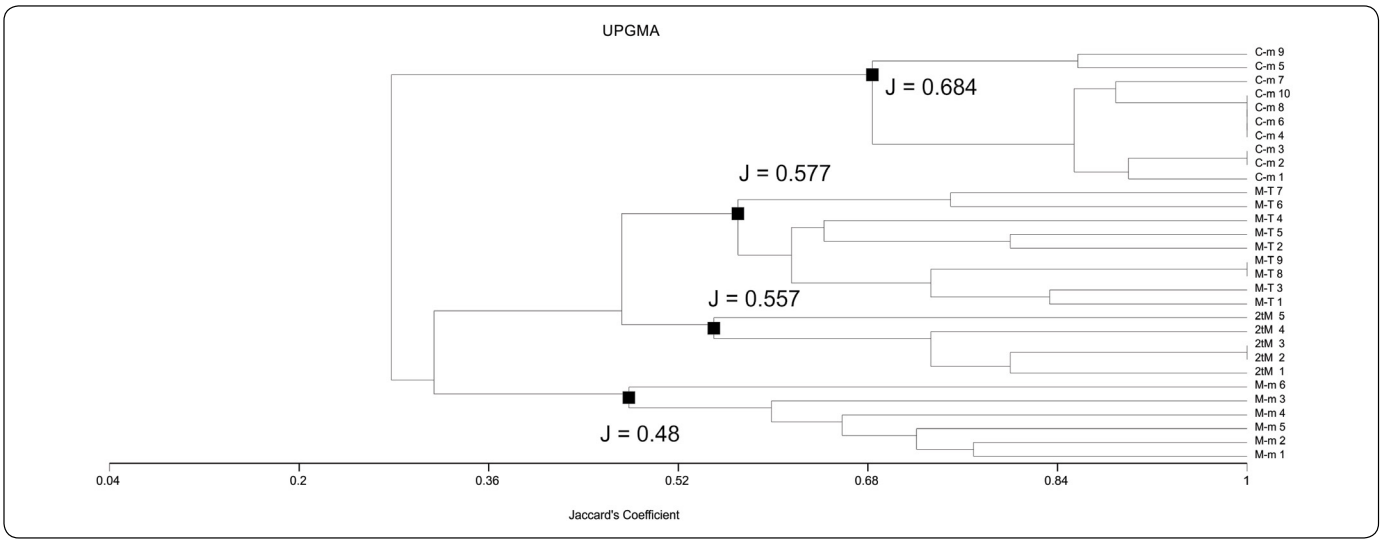

Figure 5. UPGMA—Jaccard phenogram. Note the arrangement of the samples into strong associations for the Chaetetid–microencruster (C-m) Association (J = 0.684). Two phena, with J = 0.557 and 0.577 contain the Dual-type Microbialite (2tM) and Microbialite–*Terebella* (M-T) associations, respectively. The Microbialite–microencruster (M-m) Association is grouped with a not so robust phenon, at J = 0.48. See text for further details.

DOI: 10.22201/fesz.23958723e.2019.0.171

Sample	Sample code	MIC	Dart	Prc	Mes	Cass	Epol	B-ch	Sph-C	Uv	Teth	Plv	Mcom	Apfr	Ter	Tub	Pseu	Ks	Alloc	UDTD	MESP	CEM	Total
MI - 6	M-m 1	80	5	4	0	0	0	4	0	0	0	0.033	0.033	0.033	0.033	0.033	0	0.033	6	0	0	1	100.198
MI - 10/1	M-m 2	66	9	5	0	0	0	2	0	0	0	0	0.033	0.033	0	0.033	0	0.033	14	1	0	1	98.132
JR III - 106	M-m 3	70	0	9	0	0	0	0	0	0	0	0	0.033	0.033	0.033	0.033	0	0	11	4	0	0	94.132
JR III - 32	M-m 4	72	6	1	0	0	0	0	0	0	0	0.033	0.033	0	0.033	0.033	0	0.033	13	3	0	0	95.165
MI - 7	M-m 5	70	10	1	0	0	0	5	0	0	0	0	0.033	0	0.033	0.033	0	0	5	5	0	1	97.099
MI - 9	M-m 6	54	0	0	0	0	0	0	0	0.033	0	0.033	0	0	0.033	0.033	0	0.033	12	29	0	3	98.165
M X - 5	2tM 1	85	0	0	0	0	0	0	0	0	0	0	0	0	0	0	0	0	3	1	0	5	94
M X - 8	2tM 2	76	0	0	0	0	0	0	0	0	0	0	0	0	0	0	0	0	5	2	0	10	93
M X - 2L	2tM 3	74	0	0	0	0	0	0	0	0	0	0	0	0	0	0	0	0	6	1	0	5	86
M X - 2R	2tM 4	74	0	0	0	0	0	0	0	0	0	0	0	0	0	0	0	0	5	0	0	8	87
MX-5	2tM 5	69	0	0	0	0	0	11	0	0	0	0	0	0	0	0	0	0	5	0	0	15	100
FSSA XXV 1	C-m 1	24	0	0	0	0	0	0	42	0.03	0.033	0	0	0.033	0.033	0	0.066	0.066	29	1	0	0	96.261
FSSA XXV - 7	C-m 2	26	0	0	0	0	0	0	29	0.03	0.033	0	0	0	0.033	0	0.066	0.066	39	1	0	0	95.228
FSSA XXV - 3L	C-m 3	30	0	0	0	0	0	0	37	0.03	0.033	0	0	0	0.033	0	0.066	0.066	30	1	0	0	98.228
FSSA XXV - 2L	C-m 4	19	0	0	0	0	0	0	18	0	0.033	0	0	0	0.033	0	0.066	0.066	57	4	0	0	98.198
FSSA XXV -5L	C-m 5	35	0	0	0	0	0	0	29	0	0.033	0	0	0.033	0	0	0.1	0.066	26	0	0	0	90.232
FSSA XXV - 6R	C-m 6	33	0	0	0	0	0	0	41	0	0.033	0	0	0	0.033	0	0.066	0.066	15	8	0	0	97.198
FSSA XXV 6L	C-m 7	22	0	0	0	0	0	0	36	0	0.033	0	0	0.033	0.033	0	0.033	0.066	30	4	0	0	92.198
FSSA XXV -8	C-m 8	35	0	0	0	0	0	0	34	0	0.066	0	0	0	0.033	0	0.066	0.066	22	2	0	0	93.231
FSSA XXV - 2R	C-m 9	37	0	0	0	0	0	0	30	0	0.066	0	0	0	0	0	0.066	0.066	30	0	0	0	97.198
JR Cas 27	C-m 10	26	0	0	0	0	0	0	35	0	0.066	0	0	0	0.033	0	0.066	0.033	27	6	0	0	94.198
M XL - 1	M-T 1	84	0	0	0	0	0	0	0	0	0	0	0	0	0.01	0	0	0	2	3	1	11	101.01
M XL - 2	M-T 2	90	0	0	0	0	0	0	0	0	0	0	0	0	0.01	0	0	0	1	0	0.33	9	100.34
M XL - 3	M-T 3	70	0	0	0	0	0	0	0	0	0	0	0	0	0.01	0	0	0	1	2	1	23	97.01
M XL - 4	M-T 4	72	0	0	2	0	4	0	0	0	0	0	0	0	0.01	0	0	0	1	1	0.66	19	99.67
M XVII - 5R	M-T 5	90	0	0	2	0	0	0	0	0	0	0	0	0	0.01	0	0	0	1	0	1	6	100.01
M XXI - 1	M-T 6	92	0	0	0	0	0	0	0	0	0	0	0	0	0.066	0	0	0	0	0	0.66	5	97.726
M XXI - 2	M-T 7	89	0	0	0	3	0	0	0	0	0	0	0	0	0.01	0	0	0	0	0	0.66	5	97.67
M XXI - 3	M-T 8	80	0	0	0	0	0	0	0	0	0	0	0	0	0.03	0	0	0	0	10	1.66	7	98.69
M XXI - 4	M-T 9	76	0	0	0	0	0	0	0	0	0	0	0	0	0.03	0	0	0	0	13	1	4	94.03

Table III. Summary of all associations described in this manuscript, with the most important remarks and constraints on their palaeoecology. See text for further details.

DOI: 10.22201/fesz.23958723e.2019.0.171

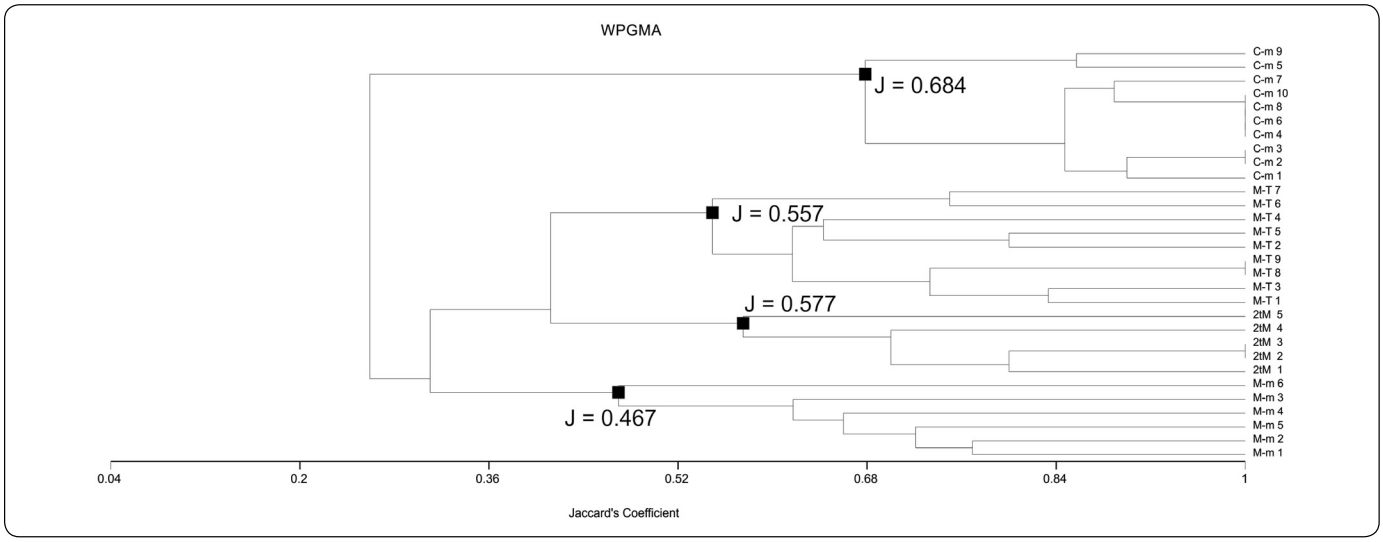

Figure 6. WPGMA—Jaccard phenogram. Note the arrangement of the samples into a strong association for the Chaetetid–microencruster (C-m) Association (J = 0.684). J values for Dual-type Microbialite (2tM) Association and Microbialite–*Terebella* (M-T) Association are inverted in comparison with the UPGMA—Jaccard phenogram (Fig. 5). M-m value is similar to Figure 5. See text for further details.

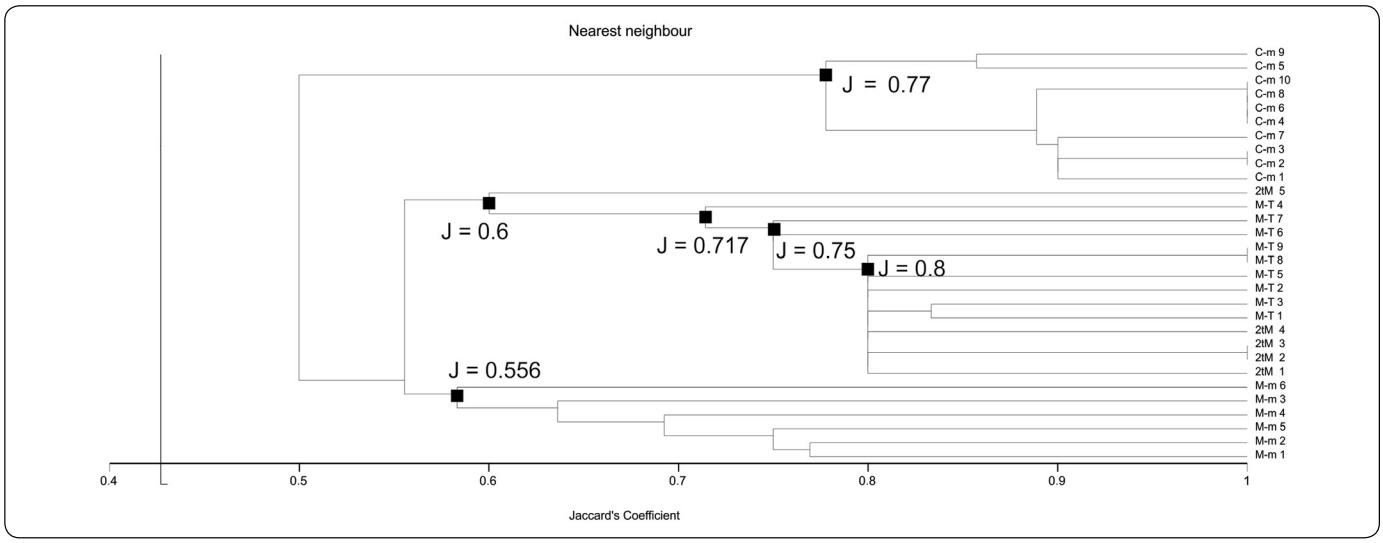

Figure 7. Nearest-Neighbour—Jaccard phenogram. Phenogram is slightly different to UPGMA—J and WPGMA—J clustering. Both Chaetetid–microencruster (C-m) and Microbialite–microencruster (M-m) phena are robust (J = 0.77 and J = 0.556, respectively). Dual-type Microbialite (2tM) and Microbialite–*Terebella* (T-M) samples are grouped within a single phenon with a J = 0.6. Note the three subordinate nodes at J= 0.717, J = 0.75 and J = 0.8. See text for further details.

Description of fossil associations

Microbialite–microencruster Association (M-m; Figures. 3a, 9; 10)

Biomorpha

Dominant component is microbialite, averaging 71%. Type II (densely clotted peloids) is the most frequent. Peloids range from 20 to 100 mm in size (average = 50 mm). Occasionally *Tubiphytes* and *Planiinvoluta*-like foraminifera (Figures. 9a, 9b), sparse nubeculariids and *Terebella* cf. *T. lapilloides* can be seen. Microbialite Type IV (stromatolite) rarely appears. While *Alpinophragmium* (Figure 9c) and *Koskinobullina socialis* (compare Sánchez-Beristain, López-Esquivel Kranksith, García-Barrera & Reitner, 2013) encrustations can only be seen associated with microbialite Type II, Type III (leiolitic fabrics) appear only associated with frequent *Microtubus* borings (Figure 10a). Pyrite framboids, between 20 and 150 mm in size, are very common (Figure 10b).

DOI: 10.22201/fesz.23958723e.2019.0.171

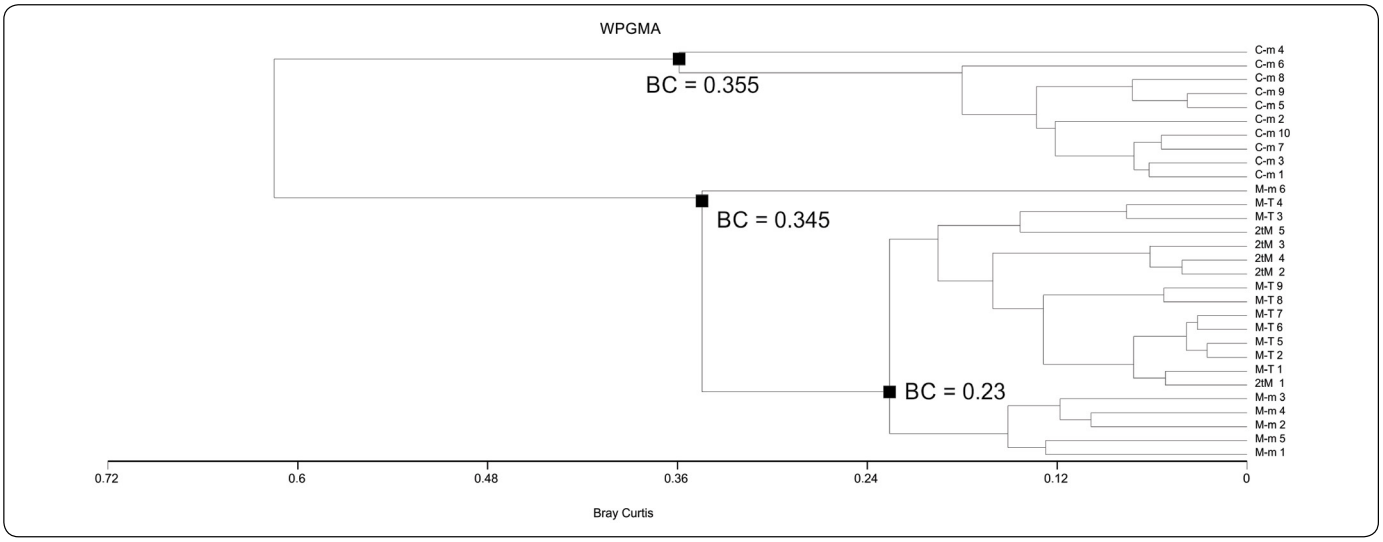

Figure 8. WPGMA—Bray Curtis phenogram. This phenogram is relatively different to the previous ones (Figs. 5-7). Chaetetid–microencruster (C-m) Association has a strong BC value (0.355). Nonetheless, a robust phenon arising at BC = 0.345 groups the three remaining associations obtained by means of both UPGMA—J and WPGMA—J, perhaps due to its lower content of microbialite. See text for further details.

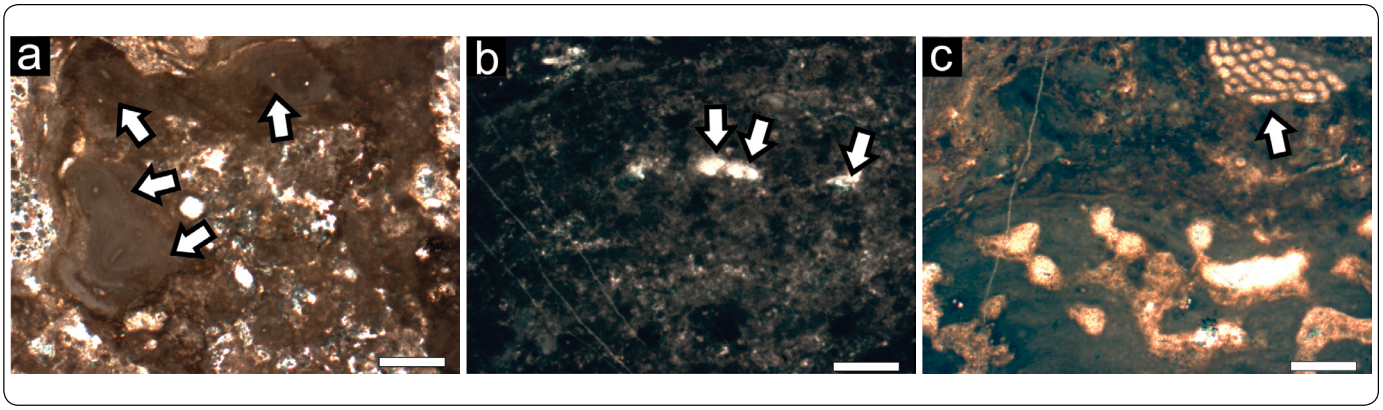

Figure 9. Microbialite – microenruster Association . a) Numerous "chimneys" of *Tubiphytes* cf. *T. obscurus* (arrows). b) *Planiinvoluta* sp. (arrows) in peloidal Type II matrix. c) *Alpinophragmium perforatum* encrustation (arrow) on automicritic substrate. Scale bar = 500 mm.

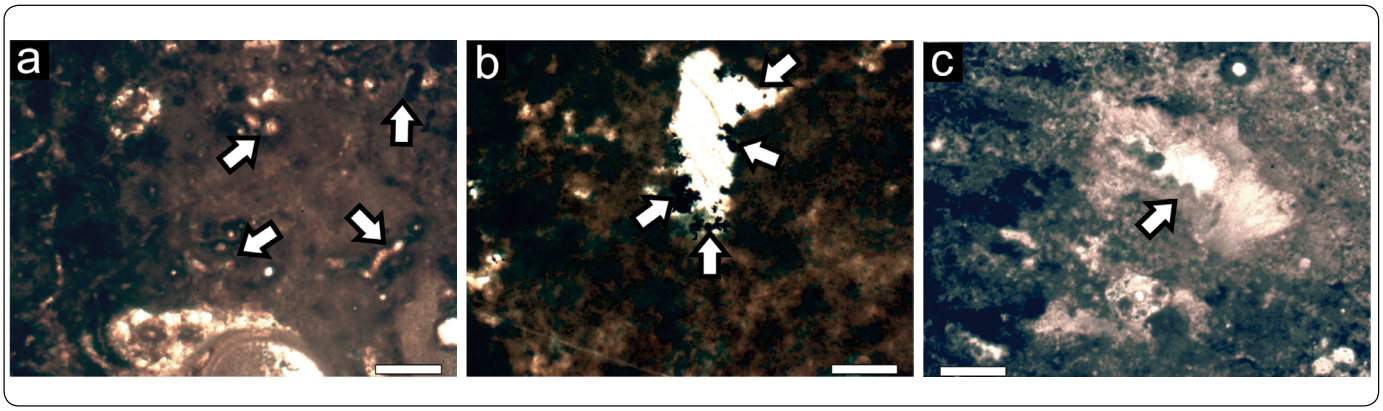

Figure 10. Microbialite – microenruster Association. a) *Microtubus communis* (arrows) associated with Type III leiolites. Scale bar = 500 mm. b) Pyrite framboids (arrows), which can be found abundantly within microbialites. Scale bar = 100 mm. c) Botryoid-like cement (arrow), possibly of aragonitic composition. Scale bar = 500 mm.

Apart from the mentioned microproblematic fossils and foraminifera, fossils are rare. They comprise only 15% of the analysed thin sections and are represented only by the coralline sponge *Precorynella* as well as by few fragments of the alga *Dendronella articulata.* It is, however, not clear if these fragments grew *in situ* or rather were allochthonously incorporated in the framework, since they appear relatively infrequently.

Associated components
Microbialites present fibrous and botryoid-like cements, presumably of aragonitic origin, which could be primary vug fillings (Figure 10c). However, the most frequent type is blocky spar cement. Nevertheless, content of cements is altogether < 1%.

Allochthonous material consists almost entirely of micrite, peloids and peloidal aggregates. In general, it proved difficult to distinguish allochthonous detritus from microbialite. However, epifluorescence analyses, which were conducted to corroborate the presence of organics, were negative in allochthonous material. Altogether, this component type accounted for no more than 13%.

Dual-type Microbialite Association (2tM; Figures 3b, 11)
Biomorpha
Skeletal fossils can only be assessed by seldom ceratoporellid chaetetids, and account for no more than 5% (Figure 11a). Microencrusters are almost absent, whereas algae lack completely. The predominant component of this association is microbialite (in average 75%), most of which is assessed to Type II, yet Type IV can also be observed. Type II can be found growing as crusts on top of chaetetid sponges and consisting of peloids with a size of ~ 30 mm, whereas Type IV has frequently associated stromatactis-type cavities and very uniform, bigger peloids, mostly ranging from 50 to 70 mm in diameter. Notable however is that stromatolite-like microbial crusts may be located growing with different directions in comparison to the chaetetids and the encrusting thrombolites (Figure 11b).

Associated components
Allochthonous sediments, which conform mudstone-wackestone fabrics, include peloids and constitute less than 5%, so they do not play an important role in the composition of this association. These sediments are found in primary vugs within the thrombolitic fabric, yet they can occasionally also be found in secondary (boring) cavities within these microbialites. Sometimes sediments include some *Tubiphytes* cf. *T. obscurus* and gastropod fragments.

Cements can mostly be found in stromatactis cavities. These include bladed calcite crystals, which are interpreted as primary based on a pink-red staining, and up to several generations of sparry calcite (Figure 11c). Overall, cements account for up to 15% of the total estimated volume of the boulders of this association, thus being one of the samples with a higher cement fraction. Other types are elsewise sparry granular calcites, which fill in stromatactis as the last generation of cements.

Chaetetid–microencruster Association (C-m; Figures 4a, 12, 13)
Biomorpha
The most noteworthy component of this association is represented by chaetetids with a sphaerulitic skeletal microstructure. They perform a baffling function (Figures 12a-b). It is also noticeable that almost no other metazoan can be found in thin sections containing this association, considering that boulders studied in this work -and especially those which contain the C-m association- reached up to 40 cm in diameter. Anyhow, these chaetetid colonies comprise up to 40% of area counting measuring.

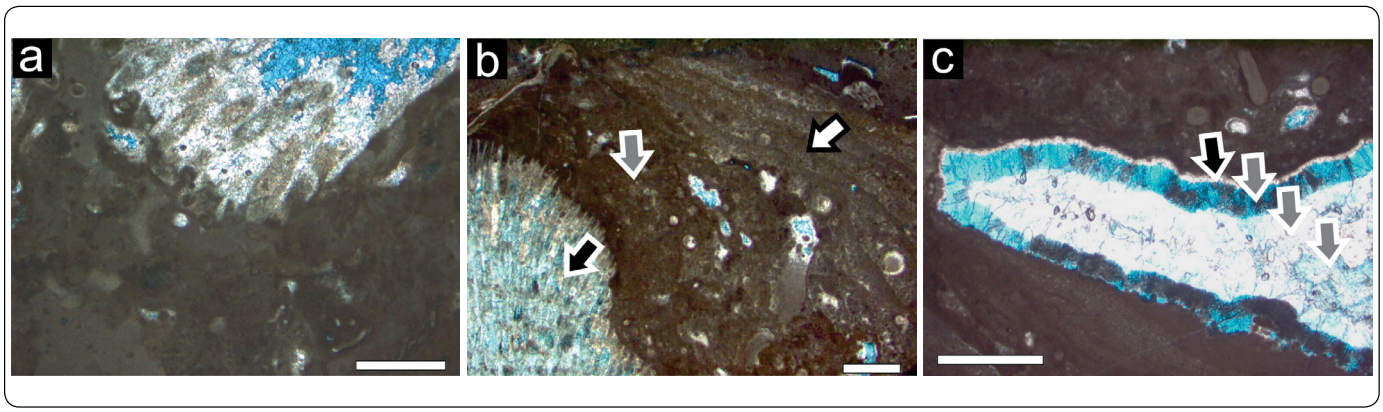

Figure 11. Dual-type Microbialite Association. a) Branch of a ceratoporellid chaetetid (upper border, center - right), one of the only sponges found as a part of this association. Scale bar = 5 mm. b) Type IV stromatolitic facies located in a different growth direction (white arrow) in comparison to a ceratoporellid sponge (black arrow) and the overlying thrombolitic crust (grey arrow). t. Scale bar = 5 mm. c) Cement succession in a stromatactis cavity. Note the four generations, which include a synsedimentary cement (black arrow) and three secondary cements (grey arrows). Scale bar = 3 mm.

DOI: 10.22201/fesz.23958723e.2019.0.171

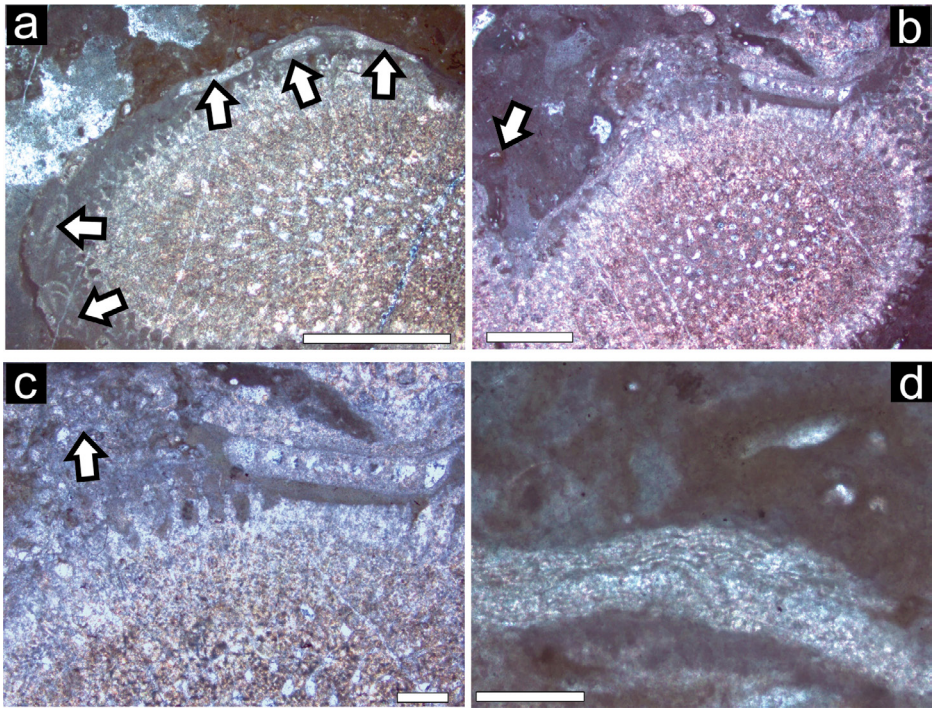

Figure 12. Chaetetid – microencruster (C-m) Association. a) Cross section of a branch of a chaetetid sponge. Note encrustations containing *Tethysocarnia cautica* (arrows) in Type III Microbialite. Scale bar = 1 mm. b) A group of microencrusters (above, center) on the surface of a chaetetid sponge. Scale bar = 1 mm. Note *Terebella* cf. *T. lapilloides* (arrow) encrusted in thrombolite. c) Enlargement of b), displaying *Koskinobullina socialis* (arrow) and *Tethysocarnia cautica* (right) 500 mm. d) *Pseudorothpletzella* – like crust associated to Type II microbialite. Scale bar = 200 mm.

Most chaetetids are covered by Type II to Type III microbialitic crusts. Altogether, however, microbialite does not reach more than 34% of area countings. Microencrusters in this association do not differ much from other associations, and include *Koskinobulina socialis* (Figure 12c), *Pseudorothpletzella* (Figure 12d), *Alpinophragmium perforatum* (Figure 13a), *Terebella* cf. *T. lapilloides* (Figures 13a, b) and *Tethysocarnia cautica* (Figure 13c). Yet here a pattern of competence for substrate is somehow clear. While on the surface of some branches only a *Pseudorothpletzella–K. socialis* association can be found, on others only individuals of *Tethysocarnia* can be seen. In addition, microbialitic fabric surrounding these tend to have a Type III fabric, whereas microbialites associated to *K. socialis* and *Pseudorothpletzella* are rather of Type II.

Associated components

Allochthonous micrite and associated detritus can be found within primary vugs formed by microbialitic growth. They account for no more than 25% of the analysed sections and can mainly be classified as mudstones. Detritus include gastropod and bivalve shells, as well as echinoid spines which can even be seen from the outer surface of some boulders. Cements have barely any importance, not even reaching 2 % of point counting in any analysed thin section.

Microbialite–*Terebella* Association (M-T; Figures 4b, 14)

Biomorpha

The main feature of this association is its complete lack of metazoan framework builders in the seven thin sections obtained from two boulders. The only identified non-microbialitic organisms are coralline algae patches, possibly belonging to *Mesophyllum.* Otherwise all thin sections in average contain more than 85% of microbialite, which is abundantly inhabited by *Terebella* cf. *T. lapilloides* (Figure 14).

Associated components

Allochthonous micrite is rather scarce (no more than 1% in average), while cements constitute more than 10%. They tend to form stromatactis-type cavities within microbialites. Microsparite accounts for no more than 1%.

Discussion

Statistical Analysis

Variations of UPGMA—J and WPGMA—J algorithms may be due to the weighting of arithmetical mean, which takes place in WPGMA, having more effect in microbialite-based associations. Withal, phenograms obtained by these two methods are very similar (Figures 5,6). This would imply that both assemblages obtained by means of UPGMA – J and WPGMA – J (2tM

DOI: 10.22201/fesz.23958723e.2019.0.171

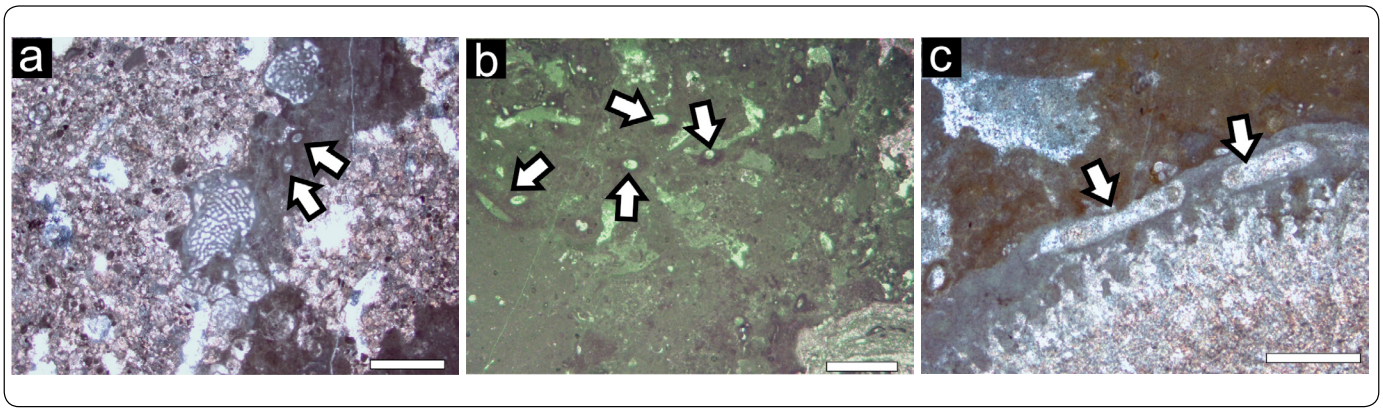

Figure 13. Chaetetid – microencruster (C-m) Association. a) ***Alpinophragmium perforatum*** **(center) and** ***Terebella*** **cf.** ***T. lapilloides*** **(arrows). Scale bar = 1 mm. b)** ***Terebella*** **cf.** ***T. lapilloides*** **tubes (arrows) immerse in Type II microbialite. Scale bar = 500 mm. c)** ***Tethysocarnia cautica*** **(arrows) encrusted in Type III microbialite Scale bar = 500 mm.**

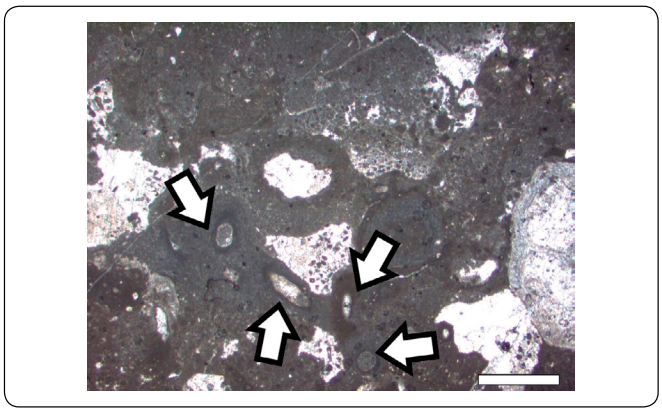

Figure 14. Microbialite –*Terebella* (M-T) Association. II. *Terebella* cf. *lapilloides* (arrows) dwelling in microbialitic substrate. Scale bar = 500 mm.

and M-T) could be grouped under the same fossil association, which is possibly because of the high content (percentage) of microbialite. Similar results could be observed in the Nearest Neighbour phenogram. The fact that all 2tM and M-T samples are grouped in a single branch could be attributed to their richness in microbialite.

For the Bray-Curtis phenogram, since a BC value of 0.345 is relatively low (McCune, Grace & Urban, 2002) the C-m Association is the most dissimilar of all four obtained by both UPGMA and WPGMA, perhaps due to its lower absolute content of microbialite, and to its higher metazoan / microencruster diversity. M-m Association (except for sample M-m 6) can also be found in a robust branch. All remaining samples (M-m 6, all 2tM and all M-T) are grouped in a single branch without nodes. As in the case for Nearest Neighbour, this could be attributed to their richness in microbialite, and furthermore to their scarceness in other components.

It must be stated that cluster analyses have rendered significant results while interpreting fossil "reef" and "reef"-like associations, especially from allochthonous or para-autochthonous samples (olistoliths), where there are not sufficient clear lateral relationships to their original depositional setting (Sánchez-Beristain & Reitner, 2016, 2018). By quantitatively determining to which extent an olistolith is composed of different components, plus using the information provided by additional features (allochthonous components and cements), it is possible to assess with certainty the percentage of each component and thus to correlate with certainty samples to a depositional environment within a "reef" or "reef"-like setting. Without performing cluster analyses, which consider both diversity and abundance of all components, it would have been easy to assume that samples with high microbialite percentages (over 75%) and even some microencrusters, would have constitute a single association. Furthermore, while comparing UPGMA—J and WPGMA—J (Figures 5, 6) with both NN—J and WPGMA—BC algorithms (Figures 7, 8), we clearly found four different associations, despite the similar microbialite percentage in three of them. This is the reason for which UPGMA—J and WPGMA—J were preferred over NN—J and WPGMA—BC, since the former two ponder diversity to a bigger extent than the latter two in samples dominated by a single component (Sokal & Michener, 1958; Legendre & Legendre, 2012).

Results presented statistically in this work are similar with those presented by Russo, Mastandrea & Baracca (1997), who reported microbialite-rich deposits in the St. Cassian outcrops in Punta Grohmann, NE Italy, and differ with the traditional metazoan-based frameworks from this *Fossillagerstätte*. According to Russo, Neri, Mastandrea & Baracca, 1997; Russo, 2005), this would represent the presence of lateral variations within the Cassian platform, which is the source for Cipit boulders.

DOI: 10.22201/fesz.23958723e.2019.0.171

Fossil associations

Microbialite–microencruster Association (M-m)

Since no considerable skeletal framework could be assessed, algae could seldom be found and microbialite is the most conspicuous component, M-m association could have originated at a deep, low energy «mud-mound» setting; probably at a subtidal level (Pratt, 1995 ; Reitner & Neuweiler, 1995). Pyrite framboids, which suggest a poorly oxygenated setting with bacterial activity (Wilkin & Barnes, 1997; Spadafora, Perri, McKenzie & Vasconcelos, 2010 ; Kershaw *et al*., 2012), further support this statement. However, stromatactis/stromatactoid cavities, which are often characteristic of these settings, are completely absent. Neuweiler & Reitner (1995) described mud mounds from the Basque Country in northern Spain that are poor in stromatactis or completely devoid of them, arguing that geopetal cavities resulting from internal sediment could be their equivalents. Nevertheless, geopetal cavities are also absent in these samples. Neuweiler (1993) described a reef setting from the Albian in northern Spain, where microbialites acted as main builders, making baffling and binding subordinate. Therefore, this possibility also remains plausible for the origin of the M-m association, especially considering the presence of aragonite cements, which, though scarce, could have a synsedimentary origin, and could thus also be associated with to the filling of primary vugs (Neuweiler & Reitner, 1995).

Similar associations were described by Aurell & Bádenas (2004) for the Kimmeridgian of NE Spain, which were interpreted as shallow ramp reef settings. Nonetheless, they noticed a high abundance of *Tubiphytes* and *Terebella* (microbial-dominated reef) during stages of relative sea-level rise. The same was noted for *Terebella* by Rodríguez-Martínez, Reitner & Mas (2010) for the Viséan of the Guadiato Valley, Córdoba, SW Spain.

Nicol (1987) found shallow coral-dominated reef communities containing *Alpinophragmium* strongly associated to *Tubiphytes* and abundant calcareous algae in the Norian of the Northern Calcareous Alps. These results are similar to those by Reijmer & Everaars (1991) from the same region, as well as for the mid- to late Jurassic of SE Sicily (Buccheri Formation; Basilone, 2018).

Regarding *Alpinophragmium,* it should however not be considered as an encruster which is diagnostic for depth conditions, since it appears to have had a broad palaeoecological distribution in reef facies (Senowbari-Daryan, Schäfer & Abate, 1983), though it is often associated to particular coral genera (Stanton & Flügel, 1987). Nevertheless, the presence and abundance of these encrusters associated to the few *Koskinobullina socialis* and, on the other side the scarcity of algae, suggest that the boulders containing the M-m association would have originated at a mid- to deep ramp, microbialite-reef subtidal setting, under low-energy conditions and perhaps poor in oxygen. However, another possibility would imply that this association originated at a cryptic, yet shallow setting, similar to those that occur at Jamaican Caribbean in the Recent (Hartman & Goreau, 1970 ; Jackson, Goreau & Hartman, 1971; Goldberg, 2013).

Dual-type Microbialite Association (2tM)

Since microbialite is the dominating component, it can be concluded that neither macroinvertebrates nor microencrusters have an important role in the palaeoenvironmental implications of this association. Microencrusters can only seldom be found on the surface of the chaetetid skeletons, or in their associated microbialitic crusts so that a deep, subtidal setting can be inferred for these chaetetids.

Moreover, it is significant that the orientation of some overlying stromatolite-like microbial growing is completely different from that of the chaetetids. This is supported by the presence of geopetal cavities with their respective infilling, which underlie this kind of microbialite. These microbialites are not colonized by any microencrusters.

Two possibilities exist for the palaeoecological interpretation of this association. On the one hand, chaetetids and associated thrombolites could have settled first in a deep/cryptic setting, followed by the establishment of a microbial community with a different growth direction, which precipitated carbonate as a layered, stromatolitic fabric.

On the other hand, it could have been possible that these stromatolites formed even at greater depths than the precursor chaetetids, especially since no associated alga could be found. In addition, stromatolites are devoid of microencrusters. This possibly indicates an oxygen-poor setting, which may indicate depths greater than 50 m (Schmid, 1996). Furthermore, deep water stromatolites are known to exist from the Mesoproterozoic (Bartley, Kah, Frank & Lyons, 2015) and have notable representatives from the Devonian (George, 1999), Mississippian (Shen & Qing, 2008) and until the Holocene (Brachert, 1999). Considering these criteria, along with the relative abundance of stromatactis, it is highly probable that the last depositional setting for this association had been related to a deep water microbialite-rich, mud mound–like environment. Though both scenarios are possible, we believe the second is more plausible. An association based on chaetetids and thombolitic microbialites could have undergone a further encrustation of stromatolites, after some boulders containing the chaetetid-thrombolite association fell from the carbonate platform front and were deposited in a deeper setting of the slope.

Chaetetid–microencruster Association (C-m)

The most remarkable feature of this association is its overall lack of calcareous algae, as well as its distinctive microencruster settling patterns. It cannot be assessed whether competence for substrate existed between *Tethysocarnia* and *Koskinobullina*.

However, it is known from present studies that substrate competence can occur between different foraminifer species (Páez, Zuniga, Valdés & Ortlieb, 2001).

The C-m association is not very diverse; nonetheless it provides sufficient criteria to make a palaeoecological preliminar assessment. It is well known that a branching growth form generally indicates low-energy conditions for bryozoans, corals and sponges (Flügel, 2010). This phenomenon has already been recorded for other Triassic localities, particularly branching corals and solenoporaceans at the Rötelwand and Adnet complexes in northern-central Austria (Schäfer, 1979), for sponges at Feichtenstein and the Gruber Reef, near Salzburg, Austria (Senowbari-Daryan, 1980), for recent sponges at the Caribbean (Wulff, 2006; James & Jones, 2015) as well as for Upper Jurassic microbialites from the Chay Peninsula in Western France (Olivier *et al.*, 2003). This type of growth in chaetetid sponges, the relative scarcity of microbialite, the lack of high-energy dwelling microencrusters, the fabric of allochthonous components, and the lack of algae may help to infer a quiet, semi-cryptic/deep (subtidal) marine setting, probably below 50 m (compare Keupp, Reitner & Salomon, 1989) that could therefore somehow be related to the *Ceratoporella-Tubiphytes* association from Sánchez-Beristain & Reitner (2018). Unfortunately, no further assessment is possible.

Microbialite–*Terebella* association (M-T)

Since microbialite is the dominant facies in all samples and framework builders are completely absent, a deep "mud mound" subtidal setting, poor in oxygen and sustained only by microbialites is the most probable interpretation. Abundant terebellids furthermore support this assumption (Wendt, Xichun & Reinhardt, 1989), since they can dwell successfully in low-oxygen conditions (Peybernes, Chablais & Martini, 2015), sometimes even in symbiosis with reducing bacteria (Guido *et al.*, 2014). It is noteworthy that no stromatolite is present, in contrast to the 2tM Association. In addition, Corallinaceae are not sufficient to give evidence of a very profound depth (Riding, 1975; Round, 1981; Pratt, 1995). Nevertheless, no further palaeoenvironmental assessment can be made. Further geochemical and sedimentological studies would be needed to approach this issue.

Conclusions

Fossil associations can be effectively obtained by means of cluster analyses. Statistical analyses results indicate that most samples described in this work are strongly dominated by microbialite. These results are similar to those presented by a previous work in another St. Cassian outcrop.

Data from microencrusters provide help to infer palaeoecological constraints which allow further separation in different associations. In the case of the Cipit boulders from the St. Cassian Formation (upper Ladinian – lower Carnian, Dolomites, NE Italy), the discovery of these associations represent a solid approach in attempting to reconstruct the palaeosynecological settings of this *Fossillagerstätte.*

Four fossil associations were obtained by clustering: Microbialite–microencruster Association, which may have either originated in a deep "mud mound" subtidal setting, or in a cryptic environment poor in oxygen; Dual-type Microbialite Association, originating initially in a cryptic-deep (subtidal) sponge-based framework with further basin-ward falling and recolonization by layered microbialites; Chaetetid–microencruster Association, coming from a quiet, semi-cryptic or deep subtidal marine setting, which would seem to modern Caribbean cryptic environments; and, Microbialite–*Terebella*, representing a deep, subtidal oxygen-poor typical microbialite-based mound? environment. Significant light influence in all associations was discarded, due to the absence of algae and to the different growth direction of some microbialitic crusts.

Being minimum at most associations, macrofossils play no significant role in framework building, leaving this niche entirely to microbialite. Microencrusters help define energy constraints for the palaeoenvironment where these associations come from.

Results from this study partially disagree with the widely accepted model for the proposed palaeoenvironment for the Cipit boulders from the St. Cassian Formation. According to this model, these boulders would have come from the Cassian platforms, which correspond to shallow "reef" and "reef"-like frameworks based on metazoans (Fürsich & Wendt, 1977; Wendt & Fürsich, 1980; Wendt, 1982; Russo, Neri, Mastandrea & Laghi, 1991). Despite coming from the most studies localities for this formation, the boulders analysed in this work present apparently little lateral variations in facies and in biotic composition in comparison with other St. Cassian microbialite-rich outcrops (Russo, Neri, Mastandrea & Baracca, 1997), and a significant one with the most known localities (Wendt, 1982). This paper thus represents the first work dealing exclusively with cryptic to deep settings inferred from fossil associations within the Cipit boulders from the Seelandalpe and Misurina.

Acknowledgments

This work was funded by the Courant Research Centre Geobiology at the Centre of Geosciences of the University of Göttingen. We are much obliged to Dr. Enrico Brutti (Bureau for Natural Parks, Autonomous Province of Bozen–South Tyrol) for having extended the authorisation to collect material at the selected localities. We are also grateful to Dr. Eric O. Walliser (Mainz), Christian Seifert and Sebastian Westphal, B.Sc. (both Göttingen) for their valuable assistance during the fieldwork. We are obliged to Edwin Aldrin Juárez-Aguilar, B. Sc. (Mexico City) for figure editing. Dr. John Hora (Göttingen) and Gabriele Schmidt (Göttingen) are greatly acknowledged for the English proofreading and final language polishing.

We would also like to thank the reviewers of this work: Dr. Beatriz Bádenas (Univertity of Zaragoza), Dr. Matías Reolid (University of Jaén) and Dr. Miguel Ángel Torres-Martínez (National Free University of Mexico), whose comments and suggestions helped improve our manuscript substantially. Finally, we would express our thank Lic. Gemma Quintero (Mexico City), for her invaluable help in the whole editing process.

References

Astibia, H., López-Martínez, N., Elorza, J. & Vicens, E. (2012). Increasing size and abundance of microbialites (oncoids) in connection with the K/T boundary in non-marine environments in the South Central Pyrenees. *Geologica Acta*, **10 (3)**, 209–226. DOI: 10.1344/105.000001770

Aurell, M. & Bádenas, B. (2004). Facies and depositional sequence evolution controlled by high-frequency sea-level changes in a shallow-water carbonate ramp. (late Kimmeridgian, NE Spain). *Geological Magazine*, **141 (6)**, 717–733. DOI: 10.1017/S0016756804009963

Bacelle, L. & Bosellini, A. (1965). Diagrammi per la stima visiva della composizione percentuale nelle rocce sedimentarie. *Annali dell'Università di Ferrara, Sezione. IX, Scienze Geologiche e Paleontologiche*, **1(3)**, 59–62.

Bartley, J.K., Kah, L.C., Frank, T.D. & Lyons, T.W. (2015). Deep-water microbialites of the Mesoproterozoic Dismal Lakes Group: microbial growth, lithification, and implications for coniform stromatolites. *Geobiology*, **13**, 15–32. DOI: 10.1111/gbi.12114

Basilone, L. (2018). *Lithostratigraphy of Sicily*. Basel: Springer.

Bizzarini, F. & Braga, G. (1978). Upper Triassic new genera and species of fair and questionable Bryozoa Chaetetida from the S. Cassiano Formation of the Dolomites (eastern Italy). *Bolletino della Società Paleontogica Italiana*, **17(1)**, 28–48.

Bosellini, A. (1991). *Geologia delle Dolomiti.* Bolzano: Casa Editrice Ahesia.

Bosellini, A., Gianolla, P. & Stefani, M. (2003). Geology of the Dolomites. *Episodes*, **26 (3)**, 181–185.

Brachert, T.C. (1999). Non-skeletal carbonate production and stromatolite growth within a Deep ocean basin (Last Glacial Maximum, Red Sea). *Facies*, **40**, 211–228. DOI: 10.1007/BF02537475

Bray, J.R. & Curtis, J.T. (1957). An ordination of upland forest communities of southern Wisconsin. *Ecological Monographs*, **27**, 325–349. DOI: 10.2307/1942268

Chan, O.W., Bugler-Lacap, D.C., Biddle, J.F., Lim, D.S., McKay, C.P. & Pointing, S.B. (2014). Phylogenetic diversity of a microbialite reef in a cold alkaline freshwater lake. *Canadian Journal of Microbiology*, **60 (6)**, 391–398. DOI: 10.1139/cjm-2014-0024

Delecat, S. & Reitner, J. (2005). Sponge communities from the Lower Liassic of Adnet (Northern Calcareous Alps, Austria). *Facies*, **51**, 385–404. DOI: 10.1007/s10347-005-0045-x

Dickson, J.A.D. (1965). A modified staining technique for carbonates in thin section. *Nature,* **205**, 587. DOI: 10.1038/205587a0

Duda, J.-P., Van Kranendonk, M.J., Thiel, V., Ionescu, D., Strauss, H., Schäfer, N. & Reitner, J. (2016). A rare glimpse of Paleoarchean life: Geobiology of an exceptionally preserved microbial mat facies from the 3.4 GA Strelley Pool Formation, Western Australia. *PLoS ONE*. DOI:10.1371/journal.pone.0147629

Dupraz, C. & Strasser, A. (2002). Nutritional modes in coral-microbialite reefs (Jurassic, Oxfordian, Switzerland): Evolution of trophic structure as a response to environmental change. *Palaios*, **17 (5)**, 449–471. DOI: 10.1669/0883-1351

Ezaki, Y., Liu, J., Nagano, T. & Adachi, N. (2008). Geobiological Aspects of the Earliest Triassic Microbialites Along the Southern Periphery of the Tropical Yangtze Platform: Initiation and Cessation of a Microbial Regime. *Palaios*, **23 (6)**, 356–369. DOI: 10.2110/palo.2007.p07-035r

Fagerstrom, J.A. (1987). *The evolution of reef communities.* New York: John Wiley and Sons.

Floquet, M., Neuweiler, F. & Léonide, P. (2012). The impact of depositional events and burial rate on carbonate-silica diagénesis in a Middle Jurassic stromatactis carbonate mud-mound, Sainte-Baume Massif, SE France. *Journal of Sedimentary Research*, **82 (7)**, 521–539. DOI: 10.2110/jsr.2012.43

Flügel, E. (2010). *Microfacies of carbonate rocks. Analysis, interpretation, application*. Berlin: Springer.

Fürsich, F.T. & Wendt, J. (1977). Biostratinomy and Palaeoecology of the Cassian Formation (Triassic) of the Southern Alps. *Palaeogeography, Palaeoclimatology, Palaeoecology*, **22**, 257–323. DOI: 10.1016/0031-0182(77)90005-0

George, A. D. (1999). Deep-water stromatolites, Canning Basin, northwestern Australia. *Palaios*, **14**, 493–505. DOI: 10.2307/3515399

Goldberg, W. M. (2013). *The biology of reefs and reef organisms*. Chicago: University of Chicago Press.

Guido, A., Jiménez, C., Achilleos, K., Rosso, A., Sanfilippo, R., Hadjioannou, L., Petrou, A., Russo, F. & Mastandrea, A. (2017). Cryptic serpulid-microbialite bioconstructions in the Kakoskali submarine cave (Cyprus, Eastern Mediterranean). *Facies*, **63(21).** DOI: 10.1007/s10347-017-0502-3

Guido, A., Mastandrea, A., Rosso, A., Sanfilippo, R., Tosti, F., Riding, R. & Russo, F. (2014). Commensal simbiosis between agglutinated polychaetes and sulfate-reducing bacteria. *Geobiology*, **12**, 265–275. DOI: 10.1111/gbi.12084

Hartman, W.D. & Goreau, T.F. (1970). Jamaican coralline sponges: their morphology, ecology and fossil relatives. *Symposia of the Zoological Society of London*, **25**, 205–243.

Heindel, K., Birgel, D., Brunner, B., Thiel, V., Westphal, H., Gischler, E., Ziegenbalg, J., Cabioch, G., Sjovall, P. & Peckmann, J. (2012). Post-glacial microbialite formation

in coral reefs of the Pacific, Atlantic, and Indian Oceans. *Chemical Geology*, **304**, 117–130. DOI: 10.1016/j.chemgeo.2012.02.009

Jaccard, P. (1912). The distribution of the flora in the alpine zone. *New Phytologist*, **11**, 37–50. DOI: 10.1111/j.1469-8137.1912.tb05611.x

Jackson, J.B.C., Goreau, T.F. & Hartman, W.D. (1971). Recent Brachiopod-Coralline Sponge Communities and Their Paleoecological Significance. *Science*, **13 (173)**, 623–625. DOI: 10.1126/science.173.3997.623

James, N. P. & Jones, B. (2015). *Origin of Carbonate Sedimentary Rocks*. West Sussex: Wiley Works.

Kershaw, S. (2017). Palaeogeographic variation in the Permian–Triassic boundary microbialites: A discussion of microbial and ocean processes after the end-Permian mass extinction. *Palaeogeography, Palaeoclimatology, Palaeoecology*, **274 (1-2)**, 1–17. DOI: 10.1016/j.jop.2016.12.002

Kershaw, S., Crasquin, S., Li, Y., Collin, P.-Y., Forel, M.-B., Mu, W., Baud, A., Wang, Y., Maurer, F. & Guo, L. (2012). Microbialites and global environmental change across the Permian-Triassic boundary: a synthesis. *Geobiology*, **10**, 25–47. DOI: 10.1111/j.1472-4669.2011.00302.x

Keupp, H. & Arp, G. (1990). Aphotische Stromatolithe aus dem süddeutschen Jura (Lias, Dogger). *Berliner geowissenschaftliche Abhandlungen A*, **124**, 3–33.

Keupp, H., Reitner, J. & Salomon, D. (1989). Kieselschwämme (Hexactinellida und „Lithistida“) aus den Cipit-Kalken der Cassianer Schichten (Karn, Südtirol). *Berliner geowissenschaftliche Abhandlungen A*, **106**, 221–241.

Legendre, P. & Legendre. L. (2012). *Numerical ecology*. Amsterdam: Elsevier Science BV.

McCune, B., Grace, J.B. & Urban, D.L. (2002). *Analysis of Ecological Communities.* Gleneden Beach: MjM Software Design.

Mietto, P., Manfrin, S., Preto, N., Rigo, M., Roghi, G., Furin, S., Gianolla, P., Posenato, R., Muttoni, G., Nicora, A., Buratti, N., Cirilli, S., Spötl, C., Ramezani, J. & Bowring, S.A. (2012). The Global Boundary Stratotype Section and Point (GSSP) of the Carnian Stage (Late Triassic) at Prati di Stuores/ Stuores Wiesen Section (Southern Alps. NE Italy). *Episodes*, **35 (3)**, 414–430.

Müller-Wille, S. & Reitner, J. (1993). Palaeobiological Reconstructions of selected sphinctozoan sponges from the Cassian Beds (Lower Carnian) of the Dolomites (Northern Italy). *Berliner geowissenschaftliche Abhandlungen Reihe E*, **9**, 253–281. DOI: 10.23689/fidgeo-771

Münster, G. (1841). Beschreibung und Abbildung der in den Kalkmergelschichten von St. Cassian gefundenen Versteinerungen. In Wissmann, H.L. & Münster, G.G. (Eds.). *Beiträge zur Geognosie und Petrefakten-Kunde des Südöstlichen Tirols vorzüglich der Schichten von St. Cassian* (pp. 25–152). Bayreuth: 4. Buchner.

Neuweiler, F. (1993). Development of Albian microbialites and microbialite reefs at marginal platform areas of the Vasco-Cantabrian Basin (Soba Reef Area, Cantabria, N. Spain). *Facies*, **29**, 231–250. DOI: 10.1007/BF02536930

Neuweiler, F. & Bernoulli, D. (2005). Mesozoic (Lower Jurassic) red stromatactis limestones from the Southern Alps (Arzo, Switzerland): calcite mineral authigenesis and syneresis-type deformation. *International Journal of Earth Sciences*, **94(1)**, 130–146. DOI: 10.1007/s00531-004-0442-3

Neuweiler, F. & Reitner, J. (1995). Epifluorescence-microscopy of selected automicrites from Lower Carnian Cipit-boulders of the Cassian Formation (Seeland Alpe, Dolomites). *Facies*, **32**, 26–28. DOI: 10.1007/BF02536864

Nicol, S. A. (1987). A down-slope Upper Triassic Reef Mound: Aflenz Limestone, Hochschwab Mountains, Northern Calcareous Alps. *Facies*, **16**, 23–36. DOI: 10.1007/BF02536747

Nose, M., Schmid, D.U. & Leinfelder, R.R. (2006). Significance of microbialites, calcimicrobes, and calcareous algae in reefal framework formation from the Silurian of Gotland, Sweden: *Sedimentary Geology*, **192 (3/4)**, 243–265. DOI: 10.1016/j.sedgeo.2006.04.009

Nützel, A., Joachimski, M. & López-Correa, M. (2010). Pronounced seasonal climatic fluctuations in the Late Triassic tropics - high-resolution oxygen isotope records from aragonitic bivalve shells (Cassian Formation, Northern Italy). *Palaeogeography Palaeoclimatology Palaeoecology*, **285**, 194–204. DOI: 10.1016/j.palaeo.2009.11.011

Olivier, N., Carpentier, C., Martin-Garin, B., Lathulliere, B., Gaillard, C., Ferry, S., Hantzpergue, P. & Geister, J. (2004). Coral-microbialite reefs in pure carbonate vesus mixed carbonate-siliciclastic depositional environments: the example of the Pagny-sur-Meuse section (Upper Jurassic, northeastern France). *Sedimentary Geology*, **205 (1-2)**, 14–33. DOI: 10.1007/s10347-004-0018-5

Olivier, N., Hantzpergue, P.**,** Gaillard, C., Pittet, B., Leinfelder, R. R., Schmid, D. U. & Werner, W. (2003). Microbialite morphology, structure and growth: a modelo f the Upper Jurassic reefs of the Chay Peninsula (Western France). *Palaeogeography, Palaeoclimatology, Palaeoecology*, **193 (3-4)**, 383–404. DOI: 10.1016/S0031-0182(03)00236-0

Páez, M., Zuniga, O., Valdés, O. J. & Ortlieb, J. (2001). Foraminíferos bentónicos recientes en sedimentos micróxicos de la bahía Mejillones del Sur (23°S), Chile. *Revista de Biología Marina y Oceanografía*, **36(2)**, 129–139. DOI: 10.4067/S0718-19572001000200002

Peybernes, C., Chablais, J. & Martini, R. (2015). Upper Triassic (Ladinian?–Carnian) reef biota from the Sambosan Accretionary Complex, Shikoku, Japan. *Facies*, **61(20)**. DOI: 10.1007/s10347-015-0446 -4

Pratt, B.R. (1995). The origin, biota and evolution of deep-water mud mounds. In Monty, C.L.V., Bosence, D.W.J., Bridges, P.D. & Pratt, B.R. (Eds.). *Carbonate mud-mounds: their origin and evolution*. *International Association of Sedimentologists, Special Publication*, **23**, 49–123. DOI: 10.1002/9781444304114.ch3

Rech, H. (1998). *Geobiologie der sogenannten "Cipit-Kalke" der Beckenfazies der Cassianer-Schichten, St. Kassian, Dolomiten*. Diplom Thesis, Universität Göttingen. 136 pp.

Reijmer, J. J. G. & Everaars, J. S. L. (1991). Carbonate platform facies reflected in carbonate basin facies (Triassic, Northern Calcareous Alps, Austria). *Facies*, **25**, 253–278. DOI: 10.1007/BF02536761

Reitner, J. (1993). Modern cryptic microbialite/metazoan facies from Lizard Island (Great Barrier Reef, Australia). Formation and concepts. *Facies*, **29**, 3–40. DOI: 10.1007/BF02536915

Reitner, J. & Neuweiler, F. (1995). Mud Mounds: A polygenetic spectrum of fine-grained carbonate buildups. *Facies*, **32**, 1–70. DOI: 10.1007/BF02536864

Reitner, J., Wilmsen, M. & Neuweiler, F. (1995). Cenomanian/Turonian sponge microbialite deep-water hardground community (Liencres, Northern Spain). *Facies*, **32**, 203–212. DOI: 10.1007/BF02536869

Riding, R. (1975). *Girvanella* and other algae as depth indicators. *Lethaia*, **8**, 173–179. DOI: 10.1111/j.1502-3931.1975.tb01310.x

Rodríguez-Martínez, M., Reitner, J. & Mas, R. (2010). Micro-framework reconstruction from peloidal-dominated mud mounds (Viséan, SW Spain). *Facies*, **56 (1)**, 139–156. DOI: 10.1007/s10347-009-0201-9

Round, F. E. (1981). *The Ecology of Algae*. Cambridge: Cambridge University Press.

Russo, F. (2005). Biofacies evolution in the Triassic platforms of the Dolomites, Italy. *Annali dell'Università degli Studi di Ferrara Museologia Scientifica e Naturalistica, Volume Speciale* **2005**, 33–45. DOI: 10.15160/1824-2707/353

Russo, F., Neri, C., Mastandrea, A. & Baracca, A. (1997). The Mud Mound Nature of the Cassian Platform Margins of the Dolomites. A Case History: the Cipit Boulders from Punta Grohmann (Sasso Piatto Massif, Northern Italy): *Facies*, **36**, 25–36. DOI: 10.1007/BF02536875

Russo, F., Neri, C., Mastandrea, A. & Laghi, G. (1991). Depositional and diagenetic history of the Alpe di Specie (Seelandalpe) fauna (Carnian, Northeastern Dolomites). *Facies*, **25**, 187–210. DOI: 10.1007/BF02536759

Saint-Martin, J.-P., Müller, P., Moissette, P. & Dulai, A. (2000). Coral microbialite environmnet in a Middle Miocene reef of Hungary. *Palaeogeography, Palaeoclimatology, Palaeoecology*, **160 (3-4)**, 179–191. DOI: 10.1016/S0031-0182(00)00065-1

Sánchez-Beristain, F. & Reitner, J. (2012). Palaeoecology of microencrusters and encrusting "coralline" sponges in Cipit boulders from the Cassian Formation (upper Ladinian-lower Carnian, Dolomites, Northern Italy). *Paläontologische Zeitschrift*, **86(2)**, 113–133. DOI: 10.1007/s12542-011-0124-y

Sánchez-Beristain, F. & Reitner, J. (2016). Palaeoecology of new fossil associations from the Cipit boulders, St. Cassian Formation (Ladinian–Carnian, Middle–Upper Triassic; Dolomites, NE Italy). *Paläontologische Zeitschrift*, **90 (2)**, 243–269. DOI: 10.1007/s12542-016-0305-9

Sánchez-Beristain, F. & Reitner, J. (2018). Four new fossil associations identified in the Cipit boulders from the St. Cassian Formation (Ladinian–Carnian; Dolomites, NE Italy). *Paläontologische Zeitschrift*, **92 (3)**, 535–556. DOI: 10.1007/s12542-017-0391-3.

Sánchez-Beristain, F., López-Esquivel Kranksith, L., García-Barrera, P. & Reitner, J. (2013). El primer registro de *Koskinobullina socialis* (Foraminífera) para el Triásico de Europa y sus implicaciones paleoecológicas. *Boletín Geológico y Minero*, **124**, 437–450.

Sánchez-Beristain, F., Schäfer, N., Simon, K. & Reitner, J. (2011). New geochemical method to characterise microbialites from the St. Cassian Formation, Dolomites, Northeastern Italy. In: Reitner, J., Quéric, N.V. & Arp, G. (Eds.). *Advances in stromatolite geobiology*, *Lecture Notes in Earth Sciences*, **131**, 411–427. DOI: 10.1007/978-3-642-10415-2_26

Schäfer, P. (1979). Fazielle Entwicklung und palökologische Zonierung zweier obertriadischer Riffstrukturen in den Nördlichen Kalkalpen („Oberrhät"-Riff-Kalke, Salzburg). *Facies*, **1**: 3–245. DOI: 10.1007/BF02536461

Schmid, D. U. (1996). Marine Mikrobialithe und Mikroinkrustierer aus dem Oberjura. *Profil*, **9**, 1–251.

Senowbari-Daryan, B. (1980). Fazielle und palöontologische Untersuchungen in oberrhätischen Riffen (Feichtenstein- und Gruberriff bei Hintersee, Salzburg, Nördliche Kalkalpen): *Facies*, **3**, 1–237. DOI: 10.1007/BF02536456

Senowbari-Daryan, B., Schäfer, P. & Abate, B. (1983). Obertriadische Riffe und Rifforganismen in Sizilien (Beiträge zur Paläontologie und Mikrofazies obertriadischer Riffe im alpin-mediterranen Raum, 27). *Facies*, **6**, 165–184. DOI: 10.1007/BF02536684

Sepkoski, J. J. Jr. (1974). Quantified coefficients of association and measurement of similarity. *Journal of the International Association for Mathematical Geology*, **6 (2)**, 135–152. DOI: 10.1007/BF02080152

Shapiro, R. (2004). Neoproterozoic-Cambrian microbialite record. *The Paleontological Society Papers*, **10**, *Neoproterozoic-Cambrian Biological Revolutions*, 5–16. DOI: 10.1017/S1089332600002308

Shen, J.-W. & Qing, H. (2008). Calcimicrobes, microbial fabrics, and algae in Mississippian Midale Beds, Midale and Glen Ewen pools, Williston Basin, Southeastern Saskatchewan. *Saskatchewan Geological Survey Summary of Investigations*, **1**, 1–10.

Simpson**,** G.L. (2007). Analogue Methods in Palaeoecology: Using the analogue Package. *Journal of Statistical Software*, **22 (2)**, 1–29. DOI: 10.18637/jss.v022.i02

Sokal, R. & Michener, C. (1958). A statistical method for evaluating systematic relationship. *University of Kansas Science Bulletin*, **38**, 1409–1438.

Spadafora, A., Perri, E., McKenzie, J. & Vasconcelos, C. (2010). Microbial biomineralization processes forming modern Ca:Mg carbonate stromatolites. *Sedimentology*, **57**, 27–40. DOI: 10.1111/j.1365-3091.2009.01083.x

Stanley, G.D. Jr. & Swart, P. (1995). Evolution of the coral-zooxanthellate symbiosis during the Triassic: A geochemical approach. *Paleobiology*, **21**, 179–199. DOI: 10.1017/S0094837300013191

Stanton, R.J. & Flügel, E. (1987). Paleoecology of Upper Triassic reefs in the Northern Calcareous Alps: reef communities. *Facies*, **16 (1)**, 175–185. DOI: 10.1007/BF02536751

Tosti, F., Mastandrea, A., Guido, A., Demasi, F., Russo, F. & Riding, R. (2014). Biogeochemical and redox record of Mid–Late Triassic reef evolution in the Italian Dolomites. *Palaeogeography, Palaeoclimatology, Palaeoecology*, **399**, 52–66. DOI: 10.1016/j.palaeo.2014.01.029

Tunis, G., Pugliese, N., Jurkovšek, B., Ogorelec, B., Drobne, K., Riccamboni, R. & Tewari, V.C. (2011). Microbialites as Markers of Biotic and Abiotic Events in the Karst District, Slovenia and Italy. In Tewari, V. & Seckbach, J. (Eds.). *STROMATOLITES: Interaction of Microbes with Sediments: Cellular Origin, Life in Extreme Habitats and Astrobiology*, **18**, (pp. 251–272) Dordrecht: Springer. DOI: 10.1007/978-94-007-0397-1_11

Turner, E.C., Narbonne, G.M. & James, N.P. (2000). Framework composition of early Neoproterozoic calcimicrobial reefs and associated microbialites, MacKenzie Mountains, N.W.T., Canada. In Grotzinger, J. P. & James, N.P. (Eds.). *Carbonate Sedimentation and Diagenesis in the Evolving Precambrian World*. *SEPM (Society for Sedimentary Geology), Special Publication*, **67**, 179–205.

Von Hauer, F. (1858). Erläuterungen zu einer geologischen Übersichtskarte der Schictgebirge der Lombardei. *Jahrbuch der Kaiserlich-Königlichen Geologischen Reichsanstalt*, **9**, 445–496.

Wahlman, G.P., Orchard, D.M. & Buijs, D.M. (2013). Calcisponge-microbialite reef facies, middle Permian (lower Guadalupian), northwest shelf margin of Permian Basin, New Mexico: *American Association of Petroleum Geologists Bulletin*, **97**, 1895–1919. DOI: 10.1306/07091313020

Webb, G. & Jell, J.S. (1997). Cryptic microbialite in subtidal reef framework and intertidal solution cavities in beachrock, Heron Reef, Great Barrier Reef, Australia: Preliminary observations. In Neuweiler, F., Reitner, J. & Monty, C. (Eds.). *Biosedimentology of microbial buildups, IGCP Project No. 380, Proceedings of 2nd Meeting Göttingen/ Germany 1996*, *Facies*, **36**, 219–223. DOI: 10.1007/BF02536885

Webb, G. & Kamber, B.S. (2000). Rare earth elements in Holocene reefal microbialites: A new shallow seawater proxy. *Geochimica et Cosmochimica Acta*, **64 (9)**, 1557–1565. DOI: 10.1016/S0016-7037(99)00400-7

Wendt, J. (1982). The Cassian Patch Reefs (Lower Carnian, Southern Alps). *Facies*, **6**, 185–202. DOI: 10.1007/BF02536685

Wendt, J. & Fürsich, F.T. (1980). Facies analysis and paleogeography of the Cassian Formation, Triassic, Southern Alps. *Rivista Italiana di Paleontologia e Stratigrafia*, **85 (3/4)**, 1003–1028.

Wendt, J., Xichun, W., & Reinhardt, J.W. (1989). Deep-water hexactinellid sponge mounds from the Upper Triassic of northern Sichuan (China). *Palaeogeography, Palaeoclimatology, Palaeoecology*, **76**, 17–29. DOI: 10.1016/0031-0182(89)90100-4

Westphal, H., Heindel, K., Brandano, M. & Peckmann, J. (2010). Genesis of microbialites as contemporaneous framework components of deglacial coral reefs, Tahiti (IODP 310). *Facies*, **56 (3)**, 337–352. DOI: 10.1007/s10347-009-0207-3

Wilkin, R. T. & Barnes, H. L. (1997). Formation processes of framboidal pyrite. *Geochimica et Cosmochimica Acta*, **61 (2)**, 323–339. DOI: 10.1016/S0016-7037(96)00320-1

Wood, R. A. (1999). *Reef evolution*. Oxford: Oxford University Press.

Wood, R. (2001). Are reefs and mud mounds really so different? *Sedimentary Geology*, **145 (3-4)**, 161–171. DOI: 10.1016/S0037-0738(01)00146-4

Wulff, J. L. (2006). Resistance *vs* recovery: morphological strategies of coral reef sponges. *Functional Ecology*, **20 (4)**, 699–708. DOI: 10.1111/j.1365-2435.2006.01143.x

Zamagni, J., Košir, A. & Mutti, M. (2009). The first microbialite - coral mounds in the Cenozoic (Uppermost Paleocene) from the Northern Tethys (Slovenia): Environmentally-triggered phase shifts preceding the PETM? *Palaeogeography, Palaeoclimatology, Palaeoecology*, **274 (1-2)**, 1–17. DOI: 10.1016/j.palaeo.2008.12.007

Zhuravlev A. Yu. (1996). Reef ecosystem recovery after the Early Cambrian extinction. In Hart M. B. (Ed.). *Biotic recovery from mass extinction events: Geological Society of London Special Publication*, **102**, 79–96. DOI: 10.1144/GSL.SP.1996.001.01.06